No. 553 January 2017

Random walk implementation of rotary diffusion in Lagrangian models of fiber orientation

O. Ahmadi, D. Kuzmin

ISSN: 2190-1767

Random walk implementation of rotary diffusion in Lagrangian models of fiber orientation

Omid Ahmadi, Dmitri Kuzmin

Institute of Applied Mathematics (LS III), TU Dortmund University, Vogelpothsweg 87, D-44227 Dortmund, Germany

Abstract

A comprehensive comparison of the Lagrangian and Eulerian frameworks for one-way coupled simulations of fiber suspension flows is performed for 2D and 3D models of orientation dynamics. An alternative approach to modeling the interactions of fibers is proposed for the Lagrangian framework. The presented methodology is based on the idea of the *random walk*, which is commonly used for modeling diffusion-like processes due to the Brownian motion of molecules. It is shown that a restriction of the random walk to the unit sphere provides an accurate description of orientation changes caused by interactions between fibers.

Keywords: `Fiber suspension flows, Lagrangian modeling, stochastic simulation, random walk, diffusion on a sphere`

1. Introduction

Fiber suspension flows play an important role in many industrial applications like papermaking or recycling. During the production processes, the orientation of fibers can significantly influence the quality of final products. Thus the rheological behavior of such flows is a topic of major interest.

The orientation change of an ellipsoidal particle immersed in a homogeneous flow depends on the local velocity gradients of the flow, which was first theoretically proved by Jeffery [1]. He derived an expression for the angular velocity of a fiber and showed that a single fiber will rotate continuously on one of an infinite set of closed orbits around the vorticity axis.

Since the hydrodynamic fiber-fiber interactions have not been considered by Jeffery, his expression is only valid for dilute suspensions and increasing the concentration leads to deviations from Jeffery's predictions. Folgar and Tucker [2] modeled the effect of interactions by introducing a rotary diffusion term, which makes Jeffery's equation valid for semi-dilute suspensions as well. More

Email addresses: `omid.ahmadi@math.uni-dortmund.de` (Omid Ahmadi), `kuzmin@math.uni-dortmund.de` (Dmitri Kuzmin)

complex models have also been proposed afterwards for the Eulerian framework; see Phelps and Tucker [3] for a comprehensive comparison of such models.

The most common way to describe the fiber orientation state is to consider a probability distribution function. In an Eulerian framework, the evolution of this function is governed by the Fokker-Planck equation [4, 5]. Since the fibers influence the flow significantly, especially in a semi-dilute or concentrated suspension, a mechanism should be found to include this effect in the flow. The probability distribution provides a complete description of fiber orientation, and the additional stresses due to the presence of fibers in the flow field are commonly modeled using even order moments of this function. The second order orientation tensor can be defined by forming dyadic products of the orientation vector and then integrating the product of these tensors with the distribution function over all possible directions. This approach to calculation of orientation tensors requires that the distribution function be already known. As the Fokker-Planck equation is mathematically complex and costly to solve, Advani and Tucker [6] proposed an evolution equation for the orientation tensor to avoid solving the equation for the distribution function. However, the overall accuracy of this model strongly depends on the modeling of the fourth order tensor which may produce nonphysical orientation states in numerical approximations [7, 8].

The advantage of the above Eulerian approach is that it is computationally more efficient than the Lagrangian approach, in which the rotary and translational motion of each fiber must be tracked individually. However, the Lagrangian approach can be more accurate, for example, in subdomains where mechanical fiber-fiber or fiber-wall interactions must be taken into account.

Although Lagrangian-based approaches were employed in many studies [9, 10, 11, 12, 13, 14, 15], to the best of our knowledge, the effect of the rotary diffusion term proposed by Folgar and Tucker [2] to model fiber interactions was taken into account in just a few Lagrangian models [16, 17].

In this work, we introduce a modification of the method developed in [17] for modeling random changes of fiber orientation due to interactions of fibers in Lagrangian models and validate it by a comprehensive comparison with Eulerian approaches for both 2D and 3D test problems. In section 2, the Jeffery equation and some approaches to computation of orientation tensors are discussed in detail for non-interacting fibers in both frameworks. After reviewing the basics of fiber interaction modeling, we present our approach for the Lagrangian framework and compare the results for some 2D and 3D simple flows to those produced by other methods.

2. Basic equations

2.1. Orientation vector

The orientation of an individual fiber (as shown in Fig. 1) is represented by a unit vector p, which can be defined in terms of two angles θ and ϕ in spherical coordinates as follows:

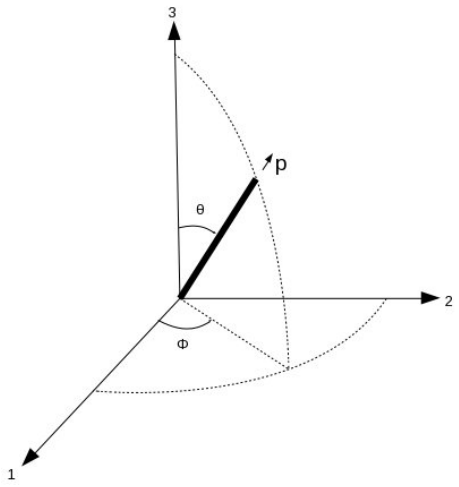

Figure 1: Orientation of a single fiber described by a unit vector p or the angles (ϕ, θ).

$$\begin{aligned} p_1 &= \sin(\theta)\cos(\phi), \\ p_2 &= \sin(\theta)\sin(\phi), \\ p_3 &= \cos(\theta). \end{aligned} \tag{1}$$

The expression obtained by Jeffery [1] for the orientation change of the unit vector in a very dilute suspension is given by

$$\dot{p} = W \cdot p + \lambda[D \cdot p - D : (p \otimes p) \cdot p], \tag{2}$$

where $D = \frac{1}{2}[\nabla u + (\nabla u)^T]$ and $W = \frac{1}{2}[\nabla u - (\nabla u)^T]$ are the strain rate tensor and the spin tensor, respectively. The shape parameter $\lambda = (r_a^2 - 1)/(r_a^2 + 1)$ depends on the aspect ratio of fibers $r_a = L/d$, where L is the fiber length and d is the diameter.

2.2. Probability distribution function

To describe the orientation of fibers, the probability distribution function $\psi(p, x, t)$ is defined as the probability of finding a fiber parallel to the orientation vector p at position x and time t. This function must satisfy

$$\psi(p) = \psi(-p), \tag{3a}$$

$$\int_{\theta=0}^{\pi} \int_{\phi=0}^{2\pi} \psi(\theta, \phi) \sin(\theta) d\theta d\phi = 1. \tag{3b}$$

In the Eulerian framework, the evolution of ψ can be described by the following Fokker-Planck equation

$$\frac{\partial \psi}{\partial t} + u \cdot \nabla \psi + \nabla_p \cdot (D_r \psi) = 0, \tag{4}$$

where D_r is a *rotary diffusivity* which will be discussed in section 3.

No evolution equation for ψ needs to be solved in the Lagrangian framework. Since the orientation of each individual fiber is known, the corresponding probability distribution function can be reconstructed using a simple postprocessing procedure. In the 2D case, an individual fiber can attain an angle in the range $(0, \pi)$ which is subdivided into m intervals. To reconstruct the distribution function ψ at a certain node, we iterate over all fibers in a neighborhood of the node and count the number of fibers located in each interval, i.e. between $p(\phi_{k-1})$ and $p(\phi_{k-1} + \frac{2\pi}{m})$, where $k = 1, \ldots, m$. Finally, the normalized distribution function for the discrete interval around $\phi_{k-\frac{1}{2}}$ is defined thus:

$$\psi(\phi_{k-\frac{1}{2}}) = \frac{\textit{number of fibers between } p(\phi_{k-1}) \textit{ and } p(\phi_{k-1} + \frac{2\pi}{m})}{\frac{2\pi}{m} \times \textit{total number of fibers}}. \tag{5}$$

It is worth mentioning that to find fibers associated with a node of the computational mesh, we consider a virtual circle (or sphere in the 3D case) around each node with the radius length of one or two mesh edge.

2.3. Orientation tensor

The influence of fibers on the local stress of the fluid can be taken into account using the second and fourth order orientation tensors [6]

$$\mathrm{A}(x,t) = \int\int_S (p \otimes p)\psi(p; x, t)dS(p) \tag{6}$$

and

$$\mathbb{A}(x,t) = \int\int_S (p \otimes p \otimes p \otimes p)\psi(p; x, t)dS(p). \tag{7}$$

To avoid the difficulty of solving the Fokker-Planck equation (4), the evolution equation

$$\frac{\partial \mathrm{A}}{\partial t} + u \cdot \nabla \mathrm{A} = (\mathrm{A} \cdot \mathrm{W} - \mathrm{W} \cdot \mathrm{A}) + \lambda(\mathrm{A} \cdot \mathrm{D} + \mathrm{D} \cdot \mathrm{A} - 2\mathbb{A} : \mathrm{D}) + D_r(6\mathrm{I} - 3\mathrm{A}) \tag{8}$$

was proposed by Advani and Tucker [6] for direct calculation of the second order orientation tensor A. Note that this model requires a suitable closure approximation for the fourth order orientation tensor $\mathbb{A}$.

To evaluate the orientation tensors in the Lagrangian framework, the integral over the unit circle (or sphere in the 3D case) in equations (6) and (7) can be split into m integrals over intervals on which the piecewise-constant reconstruction ψ is defined. We have

$$\begin{aligned} \mathrm{A}_{ij} = &\int_0^{\frac{2\pi}{m}} p_i p_j \psi(\phi)d\phi + \int_{\frac{2\pi}{m}}^{\frac{4\pi}{m}} p_i p_j \psi(\phi)d\phi \; + \cdots \\ &+ \int_{\frac{(m-1)2\pi}{m}}^{2\pi} p_i p_j \psi(\phi)d\phi \end{aligned} \tag{9}$$

and

$$\begin{aligned}\mathbb{A}_{ijql} = &\int_0^{\frac{2\pi}{m}} p_i p_j p_q p_l \psi(\phi) d\phi + \int_{\frac{2\pi}{m}}^{\frac{4\pi}{m}} p_i p_j p_q p_l \psi(\phi) d\phi + \cdots \\ &+ \int_{\frac{(m-1)2\pi}{m}}^{2\pi} p_i p_j p_q p_l \psi(\phi) d\phi.\end{aligned} \tag{10}$$

These integrals can be calculated numerically, e.g. using the midpoint rule

$$\int_{\psi_{k-1}}^{\psi_k} p_i p_j \psi(\phi) d\phi = \frac{2\pi}{m}(p_i^{mid} p_j^{mid} \psi(\phi_{k-\frac{1}{2}})), \tag{11}$$

where p^{mid} is the orientation at the midpoint of each integration interval.

It is also known that the orientation tensor can be evaluated without the necessity of computing the orientation distribution function [18]. The probability of having the orientation $\tilde{p}$ is evaluated using the formula

$$\psi(\tilde{p}) = \frac{1}{N_f} \sum_{i=1}^{N_f} \delta(\tilde{p} - p_l), \tag{12}$$

where δ is the Dirac delta function and p_l is an individual fiber in the virtual domain. This equation satisfies condition (3b), which can be shown as follows:

$$\begin{aligned}\iint_S \psi(\tilde{p}) dS(\tilde{p}) &= \iint_S \frac{1}{N_f} \sum_{i=1}^{N_f} \delta(\tilde{p} - p_l) dS(\tilde{p}) \\ &= \frac{1}{N_f} \sum_{i=1}^{N_f} \iint_S \delta(\tilde{p} - p_l) dS(\tilde{p}) \\ &= \frac{1}{N_f} \sum_{i=1}^{N_f} 1 = 1.\end{aligned} \tag{13}$$

Substituting equation (12) into equation (6) yields

$$\begin{aligned}\mathrm{A}(x,t) &= \iint_S \tilde{p}\tilde{p}\ \frac{1}{N_f} \sum_{i=1}^{N_f} \delta(\tilde{p} - p_l) dS(\tilde{p}) \\ &= \frac{1}{N_f} \sum_{i=1}^{N_f} \iint_S \tilde{p}\tilde{p}\ \delta(\tilde{p} - p_l) dS(\tilde{p}) \\ &= \frac{1}{N_f} \sum_{i=1}^{N_f} p_i p_i.\end{aligned} \tag{14}$$

The fourth order orientation tensor can be evaluated similarly:

$$\mathbb{A}(x,t) = \frac{1}{N_f} \sum_{i=1}^{N_f} p_i p_i p_i p_i. \tag{15}$$

3. Fiber-fiber interactions

Although the Jeffery equation is a fairly good model of fiber orientation in dilute suspensions, it may produce poor predictions as the concentration of fibers is increased. The reason for this lies in the hydrodynamic fiber-fiber interactions, which cause sudden reorientations of fibers as they move through the flow field and rotate with the angular velocity defined by equation (2). By observing the fiber behavior in concentrated suspensions, Folgar and Tucker [2] found that the effect of the fiber-fiber interactions can be taken into account using an additional diffusion-like term of the form

$$q = D_r \frac{1}{\psi} \nabla_p \psi, \quad D_r = C_I \dot{\gamma}, \tag{16}$$

where C_I is an empirical fiber-fiber interaction coefficient, $\dot{\gamma} = (\mathrm{D} : \mathrm{D})^{1/2}$ is the scalar magnitude of the spin tensor and the surface gradient ∇_p can be written in spherical coordinates as follows:

$$\nabla_p = \frac{\partial}{\partial \theta} e_\theta + \frac{1}{\sin(\theta)} \frac{\partial}{\partial \phi} e_\phi. \tag{17}$$

In addition to rotation with angular velocity defined by equation (2), spontaneous changes in the orientation of individual fibers may be caused by fiber-fiber interactions. Each collision results in a perturbation of the orientation angle. The changes of orientation due to these perturbations are modeled by adding the diffusion-like term q to the right-hand side of the Jeffery equation (2). In the Lagrangian framework, this term can be calculated directly (using reconstructed probability distributions) or modeled using stochastic approaches.

3.1. Direct approach

The probability distribution function ψ constructed using the above statistical approach is not smooth, particularly in complex flows, where the orientation of fibers is subject to sudden changes. The oscillatory behavior of ψ may result in a poor approximation of the diffusion term q defined by (16) if the gradient of ψ is calculated using standard discretizaion techniques such as the finite difference method. A possible remedy is the use of Fourier series (in 2D) and spherical harmonics (in 3D) to not only smooth the distribution function, but also make evaluation of the derivative more convenient.

In the 2D case ($\nabla_p = \frac{\partial}{\partial \phi} e_\phi$), the derivative that appears in the diffusion term q is discretized using the forward difference approximation

$$\frac{\partial \psi(\phi_k)}{\partial \phi} = \frac{\psi(\phi_{k+1}) - \psi(\phi_k)}{2\pi/m} \ . \tag{18}$$

Note that the discretized diffusion term is transformed to the Cartesian coordinate system ($e_\phi = -\sin\phi e_x + \cos\phi e_y$) before being added to the Jeffery equation (2).

The distribution function ψ is non-negative and satisfies condition (3a). Its Fourier series can be written in terms of the orientation angle ϕ as follows:

$$\psi_f(\phi) = a_0 + \sum_{n=1}^{\infty}(a_n \cos(n\phi) + b_n \sin(n\phi)), \tag{19}$$

where the Fourier coefficients are defined by

$$a_0 = \frac{1}{2\pi}\int_0^{2\pi} \psi(\phi)d\phi = \frac{1}{2\pi} \text{ (by 3}b\text{)}, \tag{20a}$$

$$a_n = \frac{1}{\pi}\int_0^{2\pi} \psi(\phi)\cos(n\phi)d\phi, \tag{20b}$$

$$b_n = \frac{1}{\pi}\int_0^{2\pi} \psi(\phi)\sin(n\phi)d\phi. \tag{20c}$$

It should be noted that ψ in (20) is the distribution function reconstructed using the statistical approach. Hence the Fourier coefficients can be calculated in the same way as integrals in equations (9) and (10). In view of representation (19), the derivative in the diffusion term (16) can be easily evaluated as

$$\frac{\partial \psi_f}{\partial \phi} = \sum_{n=1}^{\infty}(-a_n n \sin(n\phi) + b_n n \cos(n\phi)). \tag{21}$$

Another advantage of using the Fourier series representation is that the second and fourth order orientation tensors can be calculated from a small number of first Fourier coefficients. We have

$$\mathbb{A}_2 = \frac{\pi}{2}\begin{pmatrix} 2a_0 + a_2 & b_2 \\ b_2 & 2a_0 - a_2 \end{pmatrix}, \tag{22}$$

$$\mathbb{A}_4 = \frac{\pi}{8}\begin{pmatrix} 6a_0 + 4a_2 + a_4 & 2b_2 + b_4 & 2b_2 + b_4 & 2a_0 - a_4 \\ 2b_2 + b_4 & 2a_0 - a_4 & 2a_0 - a_4 & 2b_2 - b_4 \\ 2b_2 + b_4 & 2a_0 - a_4 & 2a_0 - a_4 & 2b_2 - b_4 \\ 2a_0 - a_4 & 2b_2 - b_4 & 2b_2 - b_4 & 6a_0 - 4a_2 + a_4 \end{pmatrix}, \tag{23}$$

as shown in detail by Lohmann [19]. However, the computational cost of the direct approach is significantly higher than that of approaches that evaluate the orientation tensors without reconstructing the underlying probability distribution function. Hence, indirect approaches are generally more efficient.

3.2. Stochastic approach

The main idea of this approach is to add stochastic perturbations to the orientation of Lagrangian fibers to achieve the same effect as using the diffusion term in the Fokker-Planck equation (4). A detailed presentation of this approach can be found in the work of Sokolichin et al. [20], who used a stochastic model of the diffusion term in the Lagrangian version of a numerical advection scheme for the volume fraction of gas in a two-phase flow model.

3.2.1. Diffusion in $\mathbb{R}^3$

In light of the above, interactions of fibers can be taken into account by solving the Jeffery equation (without any diffusion term) in $\mathbb{R}^3$ using a time stepping method that adds random perturbations to the Cartesian coordinates of the orientation vector p after each time step. This yields

$$p_i^n = p_i^n + d_i\sqrt{\Delta t}\zeta, \qquad i = 1, 2, 3, \tag{24}$$

where ζ is a random number, Δt is the constant time step and d_i is the diffusion coefficient to be defined below. The sum of perturbations must have zero mean. This can be achieved by choosing the random variable ζ to be uniformly distributed on the interval $[-a, a]$, where a is an arbitrary real number. To determine the strength (width or variance or mean square displacement) of the perturbation, we consider the diffusion equation in $\mathbb{R}^3$ with the initial condition given by the Dirac delta function. The analytical solution of this initial value problem has the form of a Gaussian distribution function:

$$A(x,t) = \prod_{i=1,2,3} \frac{1}{2\sqrt{Dt\pi}} e^{\frac{-x_i^2}{4Dt}}. \tag{25}$$

The variance of this Gaussian function is $\sigma^2 = 2Dt$, where D is the diffusion coefficient. Hence, the fibers must be perturbed in such a way that the sum of random perturbations produces the same variance as the analytical solution. Using the central limit theorem, Sokolichin et al. [20] found that the perturbations have the variance $\sigma^2 = \frac{td^2}{12}$, where d is the diffusion coefficient used in (24). This relationship guarantees that the second term on the right hand side of equation (24) has the same variance and mean value as the Gaussian function in equation (25). Whereas finding the two parameters in a Gaussian function is straightforward, the way for computing them in a discrete computation would not be clear enough. In this Lagrangian approach, a large number of fibers are perturbed at the same time. The mean of the sum of the random numbers is zero in our case, since the random variable ζ is uniformly distributed on the interval $[-a, a]$. To find the variance of the perturbations, the strength of the sum of many random numbers has to be computed using the central limit theorem. This theorem establishes that the sum of infinitely many random numbers tends toward a normal distribution. This theory and the way in which the factor $1/12$ was obtained can be explained better by a few lines of Matlab code:

```
% a = 1d array
% n = a large number of fibers
% rand = a random number uniformly distributed in [0,1]
for i=1 : n
 a(i) = (rand-0.5)
end
mean(a) % mean of the perturbations  ≃ 0
var(a) % variance of the perturbations ≃  1/12
```

Consequently, to achieve same variance as the analytical solution, the relation between the diffusion coefficients d and D must be as follows:

$$d = \sqrt{24D}. \tag{26}$$

Using this definition of d, equation (24) can be written as

$$p_i^n = p_i^n + \sqrt{12}\sqrt{2D\Delta t}\zeta, \tag{27}$$

where ζ is a random number uniformly distributed in $[-0.5, 0.5]$.

Manhart [16] pursued a similar approach in which the use of the so called Wiener process for the fibers has led to the same diffusion coefficient as the one given by (26). This approach was claimed to be equivalent to the Fokker-Planck equation. As shown above, the numerical variance associated with the diffusion coefficient (26) corresponds to an analytical solution of the diffusion equation in $\mathbb{R}^3$, whereas the diffusion term in the Fokker-Planck equation is defined using the Laplace-Beltrami operator on $\mathbb{S}^2$. However, the use of the 3D random walk is admissible in this context if normalization is performed afterwards to project the perturbed orientation vector (27) onto the surface of the unit sphere at each time step. This issue will be discussed in detail in section 4.3.

3.2.2. Diffusion on $\mathbb{S}^2$

In this work, our goal is to design a tailor-made random walk model for diffusion on $\mathbb{S}^2$ and find the corresponding diffusion coefficient. To begin with, we consider the Laplace operator written in the spherical coordinates

$$\Delta = \frac{1}{r^2}\frac{\partial}{\partial r}\left(r^2\frac{\partial f}{\partial r}\right) + \frac{1}{r^2\sin\theta}\frac{\partial}{\partial\theta}\left(\sin\theta\frac{\partial f}{\partial\theta}\right) + \frac{1}{r^2\sin^2\theta}\frac{\partial^2 f}{\partial\phi^2} \tag{28}$$

and restrict it to $\mathbb{S}^2$. Since the orientation of each fiber is described by a unit vector, the first term on the right-hand side of the above equation vanishes. Following Chen and Yu [17], we consider a second coordinate system $\{X_1', X_2', X_3'\}$ (figure 2) such that the X_3' axis is in the direction of the fiber axis OP when there is no perturbation, and X_1' is in the direction of the cross product of X_3' and X_3. In this reference frame, the Laplace-Beltrami operator is given by

$$\Delta_p = \frac{1}{\sin\Theta}\frac{\partial}{\partial\Theta}\left(\sin\Theta\frac{\partial f}{\partial\Theta}\right) + \frac{1}{\sin^2\Theta}\frac{\partial^2 f}{\partial\Phi^2}. \tag{29}$$

By analogy with the 3D random walk approach described in the previous section, the spherical coordinates of fiber orientation vectors are perturbed so as to as to reproduce the effect of the rotary diffusion term in the Fokker-Planck equation. Using Laplace-Beltrami operator for the new coordinate system and the fact that the rotation of a fiber along its main axis (here: OX_3') does not change its orientation, we find that the last term on the right-hand side of (29) vanishes too. The corresponding diffusion equation can be written as

$$\frac{\partial f}{\partial t} = \frac{D_r}{\sin\Theta}\frac{\partial}{\partial\Theta}\left(\sin\Theta\frac{\partial f}{\partial\Theta}\right). \tag{30}$$

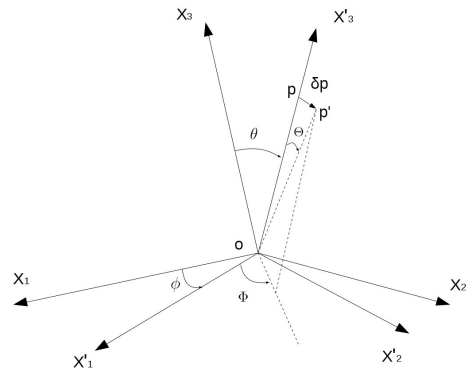

Figure 2: New coordinate system $\{X_1', X_2', X_3'\}$[17].

Assuming that the time steps are small, the variance or quadratic angular displacement can be approximated thus: $\langle \theta^2 \rangle \approx r^2\theta^2 \approx 4D_r t$ [21].

The fiber orientation vectors should be perturbed in a such way that the sum of perturbations in the angular direction θ produces the variance $\sigma^2 = 4D_r\Delta t$. The way to find the variance using the central limit theorem was discussed in the previous section. This approach yields

$$\Theta = \sqrt{12}\sqrt{4D\Delta t}\zeta. \tag{31}$$

An arbitrary perturbation of the azimuth angle is defined by

$$\Phi = 2\pi(\zeta + 0.5), \tag{32}$$

where ζ is a random number uniformly distributed on the interval $[-0.5, 0.5]$.

Let θ and ϕ denote the spherical coordinates corresponding to the Cartesian coordinates (X_1, X_2, X_3) of the orientation vector after solving the Jeffery equation without any perturbation:

$$\begin{aligned} \theta &= \arccos \frac{X_3}{\sqrt{X_1^2 + X_2^2 + X_3^2}} = \arccos \frac{X_3}{r}, \\ \varphi &= \arctan \frac{X_2}{X_1}. \end{aligned} \tag{33}$$

The following coordinate transformation converts the random shifts of the two orientation angles into small perturbations of the Cartesian coordinates:

$$\begin{bmatrix} \delta p_1 \\ \delta p_2 \\ \delta p_3 \end{bmatrix} = \begin{bmatrix} \sin\phi & \cos\theta\cos\phi & \sin\theta\cos\phi \\ -\cos\phi & \cos\theta\sin\phi & \sin\theta\sin\phi \\ 0 & -\sin\theta & \cos\theta \end{bmatrix} \times \begin{bmatrix} \sin\Theta\cos\Phi \\ \sin\Theta\sin\Phi \\ \cos\Theta \end{bmatrix} - \begin{bmatrix} \sin\theta\cos\phi \\ \sin\theta\sin\phi \\ \cos\theta \end{bmatrix}. \tag{34}$$

The definition of these perturbations in terms of angles preserves the unit norm of the orientation vector. Thus, no normalization is required in this version. It

should be noted that Chen and Yu [17] solved the simplified diffusion equation using the cumulative probability function. It led to a logarithmic expression for Θ, which differs from equation (31). However, no significant differences were observed in the results produced by the two approaches.

4. Results

In this section, a numerical study of the Lagrangian approach to fiber orientation modeling is performed for simple flows with and without taking the interaction of fibers into account. The results for the second order orientation tensor are compared to those produced by Eulerian models.

4.1. 2D homogeneous flows - without fiber interactions

In the first test case, two simple flows are chosen and the Frobenius norm is used to measure the error in the second order orientation tensor computed using the Lagrangian and Eulerian approaches. The Jeffery equation with $\lambda = \frac{99}{101}$ is solved using the explicit Euler method with the time step $\Delta t = 0.1$. The reference solution A_{ex} is computed using the formula presented by Kuzmin [22]. The velocity gradient for the *planar elongation* is defined by

$$\nabla u = \begin{pmatrix} g & 0 \\ 0 & -g \end{pmatrix}, \tag{35}$$

and for the *shear flow* it is defined by

$$\nabla u = \begin{pmatrix} 0 & g \\ 0 & 0 \end{pmatrix}, \tag{36}$$

where $g = 0.01$. The initial orientation of fibers is random, which corresponds to the isotropic probability density distribution. Figure 3 illustrates the influence of the number of fibers on the accuracy of the Lagrangian approach (14) to simulating the orientation dynamics of the elongation flow. Using more than a few thousands of fibers makes it possible to achieve small further improvements in accuracy. However, the potential benefit is hardly worth the additional cost. In the rest of this numerical study, we will use 2000 sample fibers.

In figure 4, the Lagrangian approach is compared to Eulerian models that evolve the second order orientation tensor using different closures for its fourth order counterpart. The Lagrangian simulation with 2000 sample fibers produces more accurate results than all Eulerian models except for the natural closure which yields the exact solution in the absence of fiber interactions under the assumption of isotropic initial conditions. A comparison with figure 3 reveals that the Lagrangian simulation with as few as 100 sample fibers is still more accurate than inexact Eulerian closure models. A similar comparison of the results for the shear flow leads to the same observation (see figure 5).

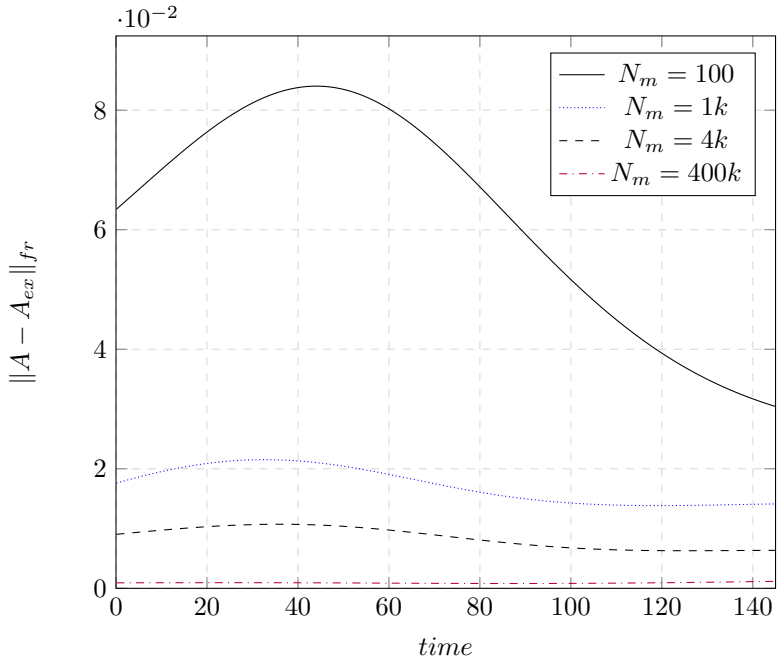

Figure 3: Influence of the number of Lagrangian fibers on the accuracy of the second order orientation tensor predictions for the 2D elongation flow.

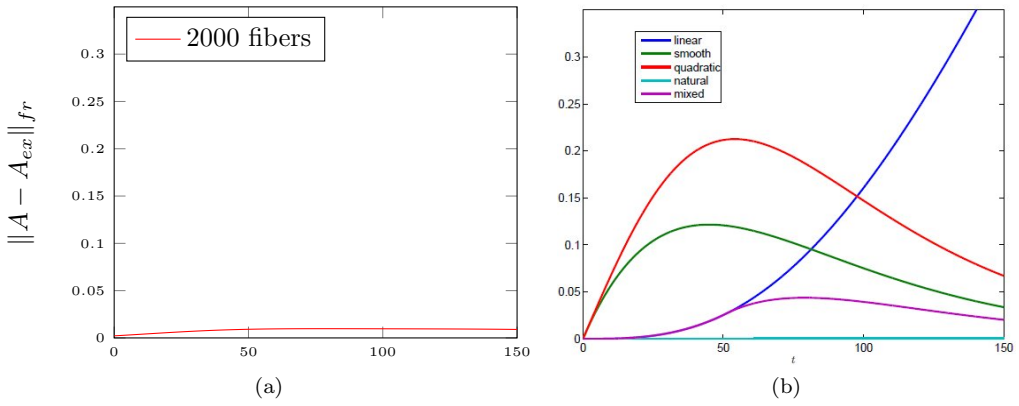

(a) (b)

Figure 4: Comparison between (a) Lagrangian simulation and (b) Eulerian approaches [22] for the 2D elongation flow.

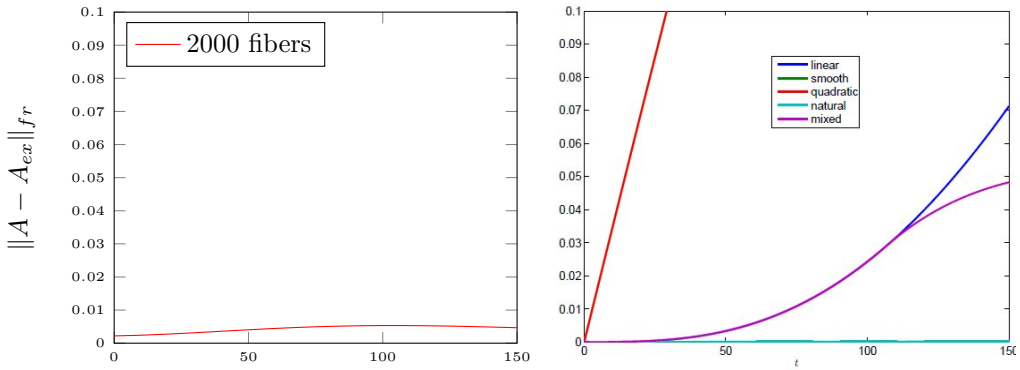

(a) (b)

Figure 5: Comparison between (a) Lagrangian simulation and (b) Eulerian approaches [22] for the 2D shear flow.

4.2. 3D homogeneous flows - without fiber interactions

Next, a numerical comparison of the Lagrangian and Eulerian modeling frameworks is performed for two simple flows in 3D. As in the 2D example, the rotary diffusion coefficient is set to zero and isotropic conditions are employed. The velocity gradient of the uniaxial elongation flow is defined by

$$\nabla u = \begin{pmatrix} 0.02 & 0.0 & 0.0 \\ 0.0 & -0.01 & 0.0 \\ 0.0 & 0.0 & -0.01 \end{pmatrix}, \tag{37}$$

and the velocity gradient of the simple shear flow is defined by

$$\nabla u = \begin{pmatrix} 0.0 & 0.05 & 0.0 \\ 0.0 & 0.00 & 0.0 \\ 0.0 & 0.0 & 0.0 \end{pmatrix}. \tag{38}$$

The results presented in figures 6 and 7 show that the Lagrangian version produces smaller errors than the Eulerian approaches under investigation also in applications to 3D simple flows.

4.3. 3D homogeneous flows - with fiber interactions

In this section, the interaction of fibers comes into play. The stochastic approaches proposed in section 3.2 are compared to each other and to the Eulerian approaches as well. Note that the figures presented in this section show the quantities of interest versus the dimensionless time parameter $t^* = tg$.

As already discussed in section 3.2.1, stochastic modeling of the diffusion term using the Cartesian random walk approach without normalization may produce orientation vectors that do not lie on the unit sphere and correspond

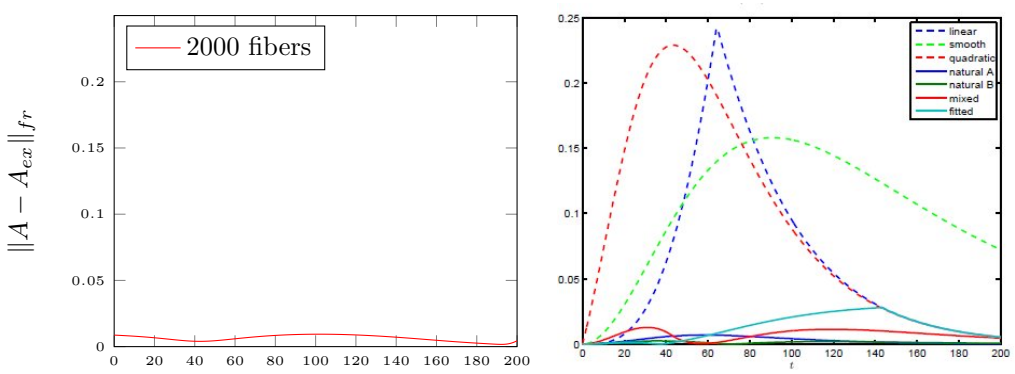

(a) (b)

Figure 6: Comparison between (a) Lagrangian simulation and (b) Eulerian approaches [22] for the 3D uniaxial elongation flow.

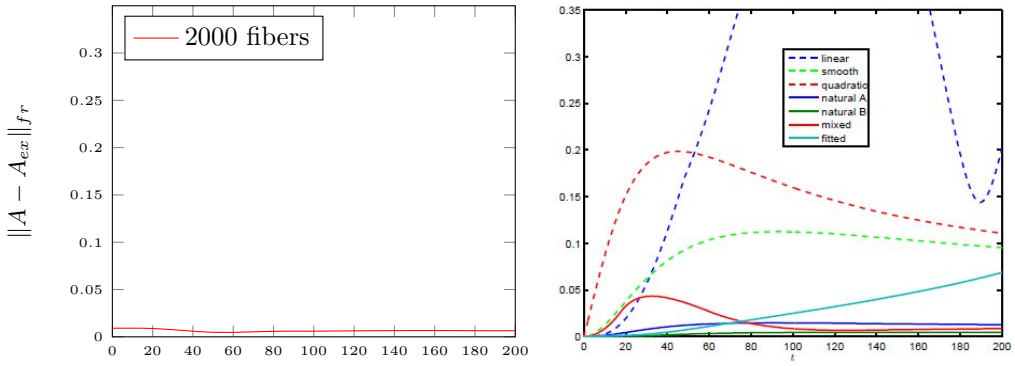

(a) (b)

Figure 7: Comparison between (a) Lagrangian simulation and (b) Eulerian approaches [22] for the 3D shear flow.

to nonphysical orientation states, as shown in figure 8. Although the Cartesian random walk approach may fail to provide a mathematically correct model of the diffusion term on $\mathbb{S}^2$, it works well in practice if the normalization of the orientation vector is performed after each time step to project the perturbed orientation vector onto the surface of the unit sphere. This is verified in figure 9, where the two stochastic approaches are compared for different interaction coefficients. Using the same seed for the random number generator, no significant differences between the approaches are observed. The $\mathbb{S}^2$ random walk version preserves the length of the orientation vector, whereas the $\mathbb{R}^3$ version

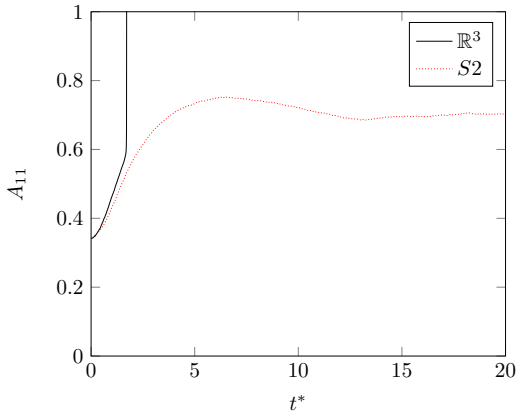

Figure 8: Comparison between the two stochastic approaches, i.e. random walks on $\mathbb{S}^2$ and in $\mathbb{R}^3$ without any normalization, $C_I = 0.01$, $\Delta t = 0.1$, $g = 0.1$.

requires normalization after each time step. It is also shown that the second order orientation tensor becomes isotropic, i.e. has the diagonal components of $\{\frac{1}{3}, \frac{1}{3}, \frac{1}{3}\}$ if the interaction coefficient is set to be greater than 1.

In figure 10, the Lagrangian approach equipped with the above stochastic models of fiber interactions is compared to different Eulerian approaches [23] for $C_I = 0.01$. The DFC curve is the reference solution. It was computed in the work of Cintra and Tucker [23] by solving the Fokker-Planck equation for the probability distribution function using a finite difference code. The other curves represent different closure models, including natural, Hinch and Leal's second composite, orthotropic fitted, and hybrid closures. While the natural closure provides the exact description of orientation dynamics in the absence of fiber interactions, the orthotropic closure yields the best predictions among the Eulerian approaches under investigation when rotary diffusion comes into play. The results of the Lagrangian simulation exhibit a very good agreement with the reference solution and are more accurate than numerical solutions obtained using the Eulerian models. By construction, the parameters of fitted closures depend on the value of the interaction coefficient C_I. Therefore, a change in the value of C_I may require the use of a different closure [23]. For example, the orthotropic fitted closure denoted by ORL in 11 was derived using polynomial fitting to numerical solutions of the Fokker-Planck equation with $C_I = 0.001$. Note that the Lagrangian approach does not require closure approximations for the fourth order tensor and the simulation results agree well with the reference solution in the whole range of the interaction coefficients.

5. Conclusions

The basic principles of one-way coupled fiber suspension flow modeling in the Lagrangian and Eulerian framework were reviewed. In the Eulerian approach,

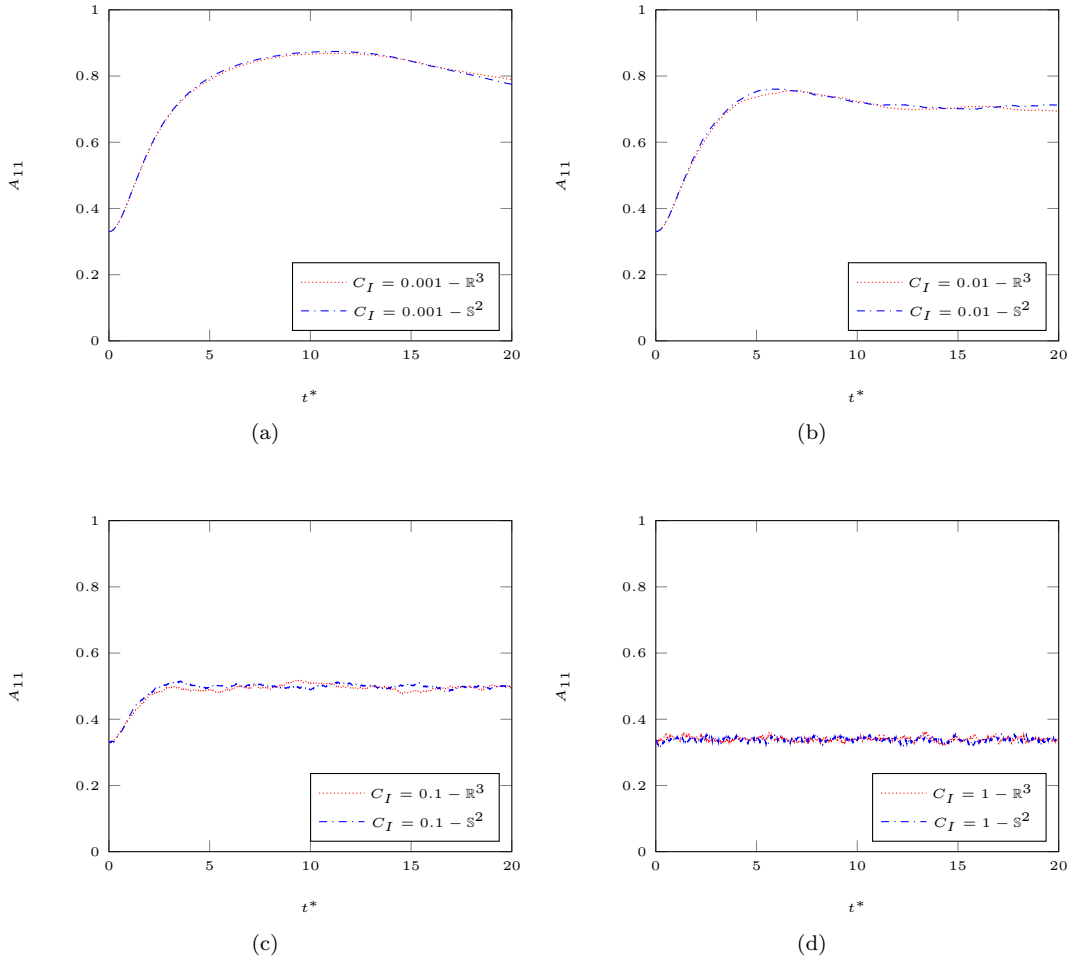

Figure 9: Comparison between the two stochastic approaches with different interaction coefficients, $\Delta t = 0.1$, $g = 0.1$, $\lambda = \frac{99}{101}$.

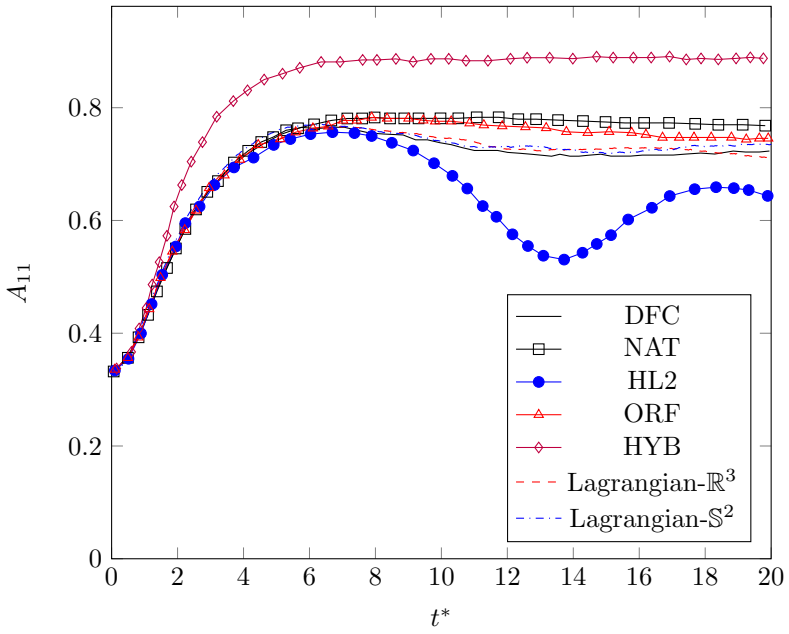

Figure 10: Comparison between the Eulerian approaches [23] and Lagrangian simulations with 2000 fibers, $C_I = 0.01$, $\lambda = 1$, $\Delta t = 0.1$, $g = 0.1$.

the second and fourth order orientation tensors can be calculated using evolution equations and closure approximations, respectively, without the necessity of knowing the position and orientation of each fiber. In contrast, each fiber is tracked individually in the Lagrangian approach, and some statistical averaging procedure is required to calculate the corresponding orientation tensors.

For a dilute suspension with negligible fiber interaction effects, Lagrangian methods prove very accurate and generally superior to most of the Eulerian approximations for 2D and 3D flows alike. As the concentration of fibers increases, fiber orientation models based on the Jeffery's equation tend to become less accurate because the local orientation states and the rheological behavior of the suspension are influenced by fiber interactions. To model this effect, Folgar and Tucker [2] added an extra diffusion term, the so-called *rotary diffusivity*, to the Jeffery equation. In this work, we modeled this diffusion term in a stochastic manner, inspired by *random walk* models of Brownian motion. The idea was verified for fibers with the aspect ratio $r_a \gg 1$.

The new stochastic approach corresponding to a random walk on $\mathbb{S}^2$, i.e., in directions orthogonal to the instantaneous orientation of rotating Lagrangian fibers, provides a more realistic model of the diffusion term than the approach based on the 3D Cartesian random walk followed by normalization after each time step. However, the latter approach produces nearly the same results in the presented numerical study. Due to some additional computations required in

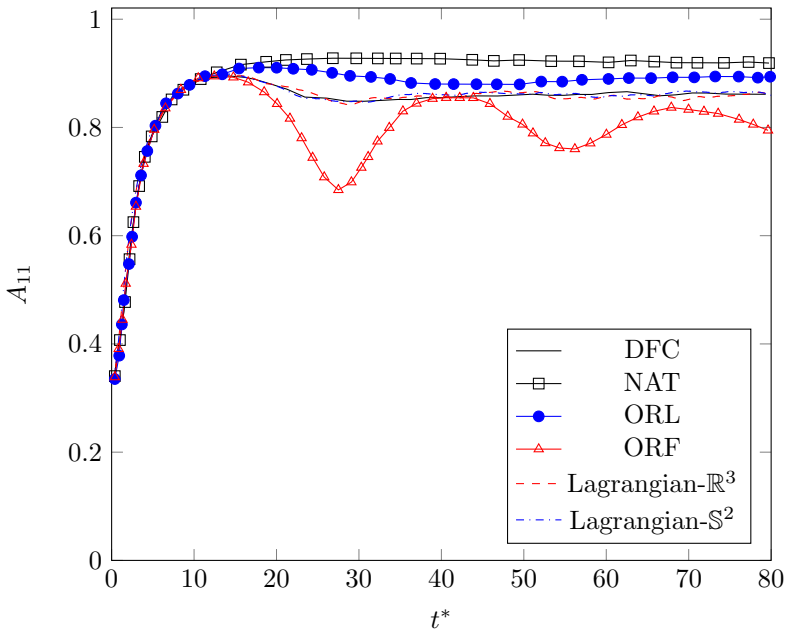

Figure 11: Comparison between the Eulerian approaches [23] and Lagrangian simulation with 2000 fibers, $C_I = 0.001$, $\lambda = 1$, $\Delta t = 0.1$ and $g = 0.1$.

the $\mathbb{S}^2$ approach, the slightly larger error of the $\mathbb{R}^3$ version may be tolerated if computational efficiency is the top priority.

Although some Eulerian approaches are well suited for modeling orientation tensors in the absence of diffusion, Lagrangian approaches are generally more accurate in the presence of the rotary diffusion term. Furthermore, the above numerical study indicates that if this term is included, Lagrangian approaches behave very well regardless of the flow pattern and of the employed interaction coefficient. Eulerian ones are quite sensitive to changes in parameter settings and no particular closure was found to be appropriate for all flows. However, the pros and cons of the two approaches require further investigation, since Eulerian simulations are generally faster than Lagrangian ones.

Acknowledgements

This research was supported by the German Research Association (DFG) under grant KU 1530/13-1.

References

[1] G. B. Jeffery, The motion of ellipsoidal particles immersed in a viscous fluid, Proceedings of the Royal Society of London A: Mathematical, Physical and

Engineering Sciences 102 (715) (1922) 161–179. doi:10.1098/rspa.1922.0078.

[2] F. Folgar, C. L. Tucker, Orientation behavior of fibers in concentrated suspensions, Journal of Reinforced Plastics and Composites 3 (2) (1984) 98–119. arXiv:http://jrp.sagepub.com/content/3/2/98.full.pdf+html, doi:10.1177/073168448400300201.
URL http://jrp.sagepub.com/content/3/2/98.abstract

[3] J. H. Phelps, C. L. T. III, An anisotropic rotary diffusion model for fiber orientation in short- and long-fiber thermoplastics, Journal of Non-Newtonian Fluid Mechanics 156 (3) (2009) 165 – 176. doi:http://dx.doi.org/10.1016/j.jnnfm.2008.08.002.
URL http://www.sciencedirect.com/science/article/pii/S0377025708001602

[4] A. D. Fokker, Die mittlere Energie rotierender elektrischer Dipole im Strahlungsfeld, Annalen der Physik 348 (1914) 810–820. doi:10.1002/andp.19143480507.

[5] G. L. II, M. Denn, D. Hur, D. Bocger, The flow of fiber suspensions in complex geometries, Journal of Non-Newtonian Fluid Mechanics 26 (3) (1988) 297 – 325. doi:http://dx.doi.org/10.1016/0377-0257(88)80023-5.
URL http://www.sciencedirect.com/science/article/pii/0377025788800235

[6] S. G. Advani, C. L. Tucker, The use of tensors to describe and predict fiber orientation in short fiber composites, Journal of Rheology 31 (8) (1987) 751–784. doi:http://dx.doi.org/10.1122/1.549945.
URL http://scitation.aip.org/content/sor/journal/jor2/31/8/10.1122/1.549945

[7] B. E. Verweyst, C. L. Tucker, Fiber suspensions in complex geometries: Flow/orientation coupling, The Canadian Journal of Chemical Engineering 80 (6) (2002) 1093–1106. doi:10.1002/cjce.5450800611.
URL http://dx.doi.org/10.1002/cjce.5450800611

[8] B. Reddy, G. Mitchell, Finite element analysis of fibre suspension flows, Computer Methods in Applied Mechanics and Engineering 190 (1819) (2001) 2349 – 2367. doi:http://dx.doi.org/10.1016/S0045-7825(00)00238-3.
URL http://www.sciencedirect.com/science/article/pii/S0045782500002383

[9] K. A. Ericsson, S. Toll, J.-A. E. Mø anson, The two-way interaction between anisotropic flow and fiber orientation in squeeze flow, Journal of Rheology 41 (3) (1997) 491–511. doi:http://dx.doi.org/10.1122/1.550833.
URL http://scitation.aip.org/content/sor/journal/jor2/41/3/10.1122/1.550833

[10] K. Chiba, K. Nakamura, Numerical solution of fiber suspension flow through a complex channel, Journal of Non-Newtonian Fluid Mechanics 78 (23) (1998) 167 – 185. doi:http://dx.doi.org/10.1016/S0377-0257(98)00067-6.
URL http://www.sciencedirect.com/science/article/pii/S0377025798000676

[11] K. Chiba, K. Yasuda, K. Nakamura, Numerical solution of fiber suspension flow through a parallel plate channel by coupling flow field with fiber orientation distribution, Journal of Non-Newtonian Fluid Mechanics 99 (23) (2001) 145 – 157. doi:http://dx.doi.org/10.1016/S0377-0257(01)00118-5.
URL http://www.sciencedirect.com/science/article/pii/S0377025701001185

[12] K. Chiba, F. Chinesta, Numerical simulation of flow kinematics and fiber orientation for multi-disperse suspension, Rheologica Acta 45 (1) (2005) 1–13. doi:10.1007/s00397-004-0431-2.
URL http://dx.doi.org/10.1007/s00397-004-0431-2

[13] K. Chiba, Eco-strategy of numerical simulation for fiber assembly orientation in an abrupt planar contraction flow, International Journal of Material Forming 3 (2) (2010) 1303–1312. doi:10.1007/s12289-009-0414-z.
URL http://dx.doi.org/10.1007/s12289-009-0414-z

[14] C. Eberhardt, A. Clarke, Fibre-orientation measurements in short-glass-fibre composites. part I: automated, high-angular-resolution measurement by confocal microscopy, Composites Science and Technology 61 (10) (2001) 1389 – 1400. doi:http://dx.doi.org/10.1016/S0266-3538(01)00038-0.
URL http://www.sciencedirect.com/science/article/pii/S0266353801000380

[15] J. J. J. Gillissen, B. J. Boersma, P. H. Mortensen, H. I. Andersson, The stress generated by non-Brownian fibers in turbulent channel flow simulations, Physics of Fluids 19 (11). doi:http://dx.doi.org/10.1063/1.2800041.
URL http://scitation.aip.org/content/aip/journal/pof2/19/11/10.1063/1.2800041

[16] M. Manhart, Rheology of suspensions of rigid-rod like particles in turbulent channel flow, Journal of Non-Newtonian Fluid Mechanics 112 (23) (2003) 269 – 293. doi:http://dx.doi.org/10.1016/S0377-0257(03)00105-8.
URL http://www.sciencedirect.com/science/article/pii/S0377025703001058

[17] Y. K. Chen, C. P. Yu, Monte Carlo simulation of fiber orientation in a shear flow with Brownian rotation, Aerosol Science and Technology 16 (4) (1992)

255–264. arXiv:http://dx.doi.org/10.1080/02786829208959554, doi:10.1080/02786829208959554.
URL http://dx.doi.org/10.1080/02786829208959554

[18] A. Moosaie, et al., Direct numerical simulation of turbulent drag reduction by rigid fiber additives, Fachgebiet Hydromechanik, 2011.

[19] C. Lohmann, Galerkin-Spektralverfahren für die Fokker-Planck-Gleichung, Springer-Spektrum, 2016, https://link.springer.com/book/10.1007/978-3-658-13311-5.

[20] A. Sokolichin, G. Eigenberger, A. Lapin, A. Lübbert, Dynamic numerical simulation of gas-liquid two-phase flows Euler/Euler versus Euler/Lagrange, Chemical Engineering Science 52 (4) (1997) 611 – 626. doi:http://dx.doi.org/10.1016/S0009-2509(96)00425-3.
URL http://www.sciencedirect.com/science/article/pii/S0009250996004253

[21] T. Carlsson, T. Ekholm, C. Elvingson, Algorithm for generating a Brownian motion on a sphere, Journal of Physics A: Mathematical and Theoretical 43 (50) (2010) 505001.
URL http://stacks.iop.org/1751-8121/43/i=50/a=505001

[22] D. Kuzmin, Planar and orthotropic closures for orientation tensors in fiber suspension flow models, Tech. rep., Fakultät für Mathematik, TU Dortmund, Ergebnisberichte des Instituts für Angewandte Mathematik, Nummer 545 (Jul. 2016).

[23] J. S. Cintra, C. L. Tucker, Orthotropic closure approximations for flow-induced fiber orientation, Journal of Rheology 39 (6) (1995) 1095–1122. doi:http://dx.doi.org/10.1122/1.550630.
URL http://scitation.aip.org/content/sor/journal/jor2/39/6/10.1122/1.550630